Validation of a combined CFD/FEM methodology for the evaluation of thermal load acting on aluminum alloy pistons through hardness measurements in internal combustion engines

G. Cantore, M. Giacopini, R. Rosi, A. Strozzi
University of Modena & Reggio Emilia (Italy), Department of Mechanical and Civil Engineering

P. Pelloni, C. Forte, M. Achiluzzi, G. M. Bianchi
University of Bologna (Italy), DIEM Department

L. Ceschini, A. Morri
University of Bologna (Italy), SMETEC Department

ABSTRACT

This work presents the results of a multidisciplinary research project, carried out in close collaboration with Ducati Motor Holding S.p.A., for the development of an integrated methodology to design engine components in aluminum alloy under high thermal loads. The results refer to the study of an AA2618 (Al-Cu-Mg) alloy piston for high performance motorcycle engines. The piston has been selected as the pilot component for the development and validation of an advanced Fluid Dynamics (CFD) and Finite Element (FE) simulation methodology for the prediction of the inner thermal diffusion. The subsequent validation has been achieved through both the mechanical and microstructural characterization of the component. The methodology here presented consists of close interaction between fluid-dynamics (CFD) simulations of the combustion process and Finite Element (FEM) simulations of the thermal diffusion inside the components. Combustion is the main engine heat source and is simulated by means of a three-dimensional CFD code for reactive flows (FIRE v2008-AVL), with the use of advanced combustion (ECFM) and wall interaction models. The temperature map on the surfaces is based on the results of the iteration with FEM simulation of thermal diffusion. The FEM model used for the diffusion analysis receives the results of combustion analysis as input. Two different methods have been tested for the transfer of the CFD thermal load to the FEM models: a) imposition on the piston crown of a spatial distribution of heat flux averaged over the mean engine cycle; b) imposition on the piston crown of both heat flux coefficients and temperatures. The latter option allows the reduction of the number of iterations for the convergence of the thermal map inside the piston. The dissipation of the thermal load is accomplished by applying heat coefficients and temperatures, on the remaining parts of the piston surface. The validation of the CFD/FEM methodology is carried out through hardness measurements in different piston locations after bench tests. The identification of the hardness curves, as a function of temperature and time, for the T6 heat-treated AA2618 allowed the assessment of the local temperature reached by the component from the knowledge of the operating time of the engine and local hardness.

RIASSUNTO

In questo lavoro si presentano i risultati di un progetto di ricerca multidisciplinare, realizzato in collaborazione con l'azienda Ducati Motor Holding S.p.A., mirato allo sviluppo di una metodologia integrata di progettazione di componenti motore in lega d'alluminio, sollecitati ad elevate temperature. I risultati fanno riferimento allo studio di un pistone in lega AA2618 (Al-Cu-Mg) per motore motociclistico ad elevate prestazioni. Il pistone è stato identificato come il componente pilota per lo sviluppo e la validazione di una metodologia avanzata di simulazione CFD-FEM, finalizzata ad ottenere una corretta previsione del campo termico che si sviluppa all'interno del componente stesso, con successiva validazione dei risultati ottenuti attraverso una caratterizzazione microstrutturale e meccanica del componente. La metodologia sviluppata nel presente lavoro prevede l'interazione tra simulazioni CFD del processo di combustione e simulazioni FEM di diffusione termica nei componenti. La combustione è la principale sorgente di calore nel motore e viene simulata con un codice CFD tridimensionale di flussi reattivi (FIREv2008-AVL), utilizzando modelli avanzati di combustione (ECFM) e di previsione del calore perso a parete. L'imposizione della temperatura a parete viene fissata sulla base delle iterazioni effettuate con le simulazioni FEM di diffusione termica nei componenti motore. Il modello utilizzato per le analisi FEM di diffusione del calore riceve come input i risultati delle analisi di combustione. Sono stati valutati due diversi metodi per il trasferimento dei carichi termici dai modelli CFD ai modelli FEM: a) si è applicata sul cielo del pistone una distribuzione spaziale del flusso termico puntuale mediato sul ciclo motore; b) si è applicata, sul cielo del pistone, una combinazione di coefficienti di scambio termico e temperature dei gas, variabili spazialmente. Si è osservato come l'impiego di questo secondo metodo minimizzi il numero di iterazioni utili per ottenere la convergenza del campo termico calcolato all'interno del pistone. Lo smaltimento del calore attraverso le altre superfici del pistone è stato poi modellato applicando coefficienti di scambio termico e temperature di riferimento opportunamente calcolati. La validazione della metodologia CFD/FEM è stata effettuata attraverso misure di durezza in varie zone del pistone, dopo prove al banco. La determinazione sperimentale delle curve di degrado (durezza in funzione di temperatura e tempo di permanenza) e quindi delle mappe isodurometriche della lega AA2618 ha permesso, infatti, di valutare la temperatura puntuale raggiunta dal componente a partire dalla conoscenza del tempo di funzionamento del motore e della durezza locale.

KEYWORDS

Piston, AA2618, hardness curves, finite element, combustion, heat flux

INTRODUCTION

The design requires a correct balance between performance optimization and a reasonable level of reliability for the development of high performance internal combustion engines.

An accurate evaluation of the temperature map of the piston surfaces adjoining the combustion chamber allows better control of the origin of abnormal combustion (i.e. pre-ignition, knock) and, at the same time, more efficient combustions. The main heat source of the engine is the combustion of the mixture inside the chamber: the estimation of the thermal load acting on the components is very difficult in such a narrow space, due to the complexity of the phenomena involved and the limited time scales.

The piston is one of the most heavily stressed engine components, since it is subjected to both thermal and mechanical loads. The maximum sustainable temperature value of the piston at any point must not be higher than 66% of the onset temperature for melting of the alloy [1]. The induced thermal strains heavily influence the capability to control the friction between the piston and liner.

The main goal of this research activity is to validate a combined FEM/CFD methodology for the evaluation of thermal loads acting on high performance engine pistons, by means of hardness measurements. As the phenomena are so complex, specialized knowledge is required; in this work a simulation methodology is presented, which iteratively uses fluid-dynamics (CFD) and Finite Element (FEM) tools, validated against experimental analysis of hardness measurements and microstructural evaluations.

EXPERIMENTAL SETUP AND METHODOLOGY

The analysis platform has been applied to a high performance Ducati engine under extremely critical configurations for the reliability of the engine (speed 8000rpm, full load).

The simulation of the combustion process has been carried out by means of a three dimensional CFD code of reactive flows (FIREv2008-AL), with the use of advanced combustion (ECFM) and wall function models. The wall temperature is imposed by basing the results of the iteration between the CFD and FEM simulations. The FEM model for the diffusion analysis uses the results of the combustion analysis as input and applies simplified heat exchange models for interaction with the other engine components.

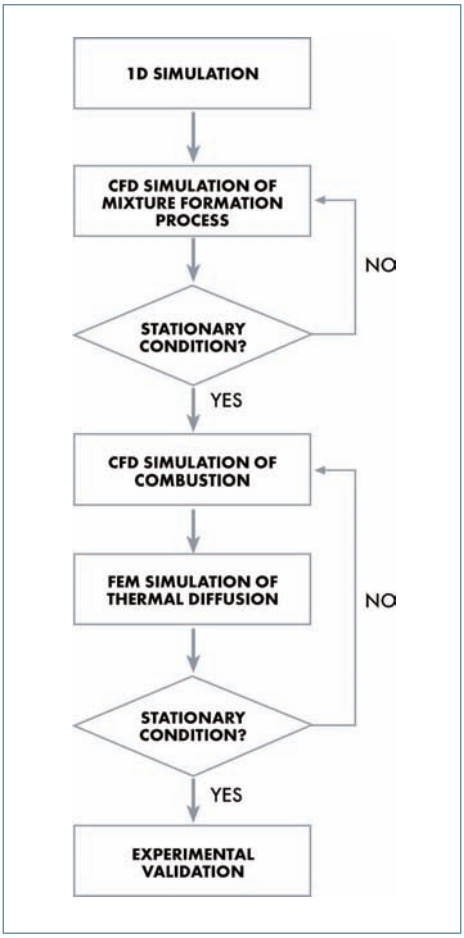

Fig. 1: Methodology flow chart.

The methodology is validated by hardness tests on the piston crown. Earlier evaluation of the hardness curves of the T6 heat treated 2618 Al alloy, as a function of the temperature and time is needed. They were obtained by annealing samples directly extracted from the pistons, between 200-320°C, for a time duration of 2 minutes to 7 days.

The flow chart in Fig. 1 briefly describes the methodology, with the CFD/FEM iteration and subsequent experimental validation.

CFD ACTIVITY

The main aim of the CFD activity is the simulation of the combustion process of the mean representative cycle, in order to estimate the heat flux to the wall in the combustion chamber.

MIXTURE FORMATION PROCESS

The simulation of the combustion process is closely related to the fluid dynamic conditions in the chamber: preliminary CFD activity is needed for the correct simulation of the intake stroke. In high performance engines (like the Ducati engine under analysis) the pressure wave oscillations in the intake duct are used for overcharging: a correct reconstruction of the dynamics of the intake duct is obtained by conveniently activating the simulation domain. This is accomplished by using the results of 1D simulation of the whole engine made by Ducati as boundary conditions. Monodimensional CFD codes can be used to simulate the fluid dynamics of the engine

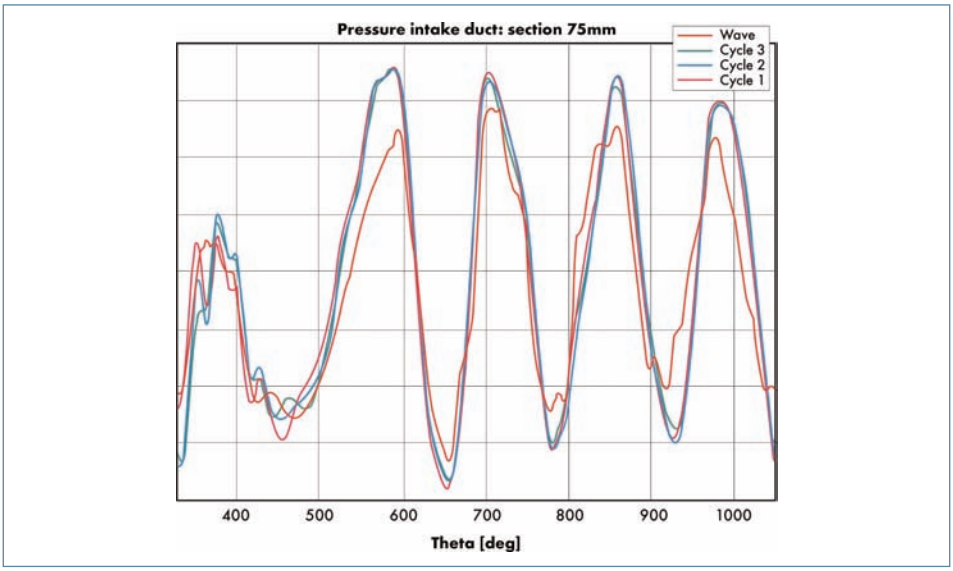

Fig. 2: Pressure wave evolution in section of the intake duct.

with little need for computational data.
The simulation of the intake stroke is carried out with a FIRE v2008.2 (AVL) code on a simplified domain: multi-cycle simulation of the intake duct connected to a plenum in order to obtain the real resonance engine behavior. The standard k-ε turbulence model has been used together with Hybrid Wall Treatment. The initial condition in the intake duct is taken from mono-dimensional results, but multi-cycle simulation is needed to reach a stationary condition. The evolution of the pressure traces on a test section is plotted in Fig. 2 for the three engine cycles simulated: comparison with 1D results shows good reconstruction of the pressure peak phases. The difference in the amplitude of the waves can be ascribed to the better capability of Fire to simulate the three-dimensionality of the reflection of the waves at the trumpet. The fluid-dynamic characteristics at the inlet valve closing (IVC) have been used for the evaluation of cyclic convergence: at IVC, mass, turbulence and the tumble motion of the third cycle are almost the same as the previous cycle.

COMBUSTION STEP 1

The simulation of the combustion phase starts with the imposition of the stationary conditions reached at IVC in the previous section. The combustion model used in the simulation (ECFM, Extended Coherent Flamelet Model, Colin et Al, 2003, [2]) is characterized by a simplified twostep chemical reaction and by the imposition of the dissociation CO-CO_2, according to the Meintjes and Morgan model.
The two-steps reactions are:

$$C_nH_mO_k + \left(n + \frac{m}{4} - \frac{k}{2}\right) O_2 \rightarrow nCO_2 + \frac{m}{2} H_2O$$

$$C_nH_mO_k + \left(\frac{n}{2} - \frac{k}{2}\right) O_2 \rightarrow nCO_2 + \frac{m}{2} H_2O$$

The chemical reactions involved in the post flame equilibrium scheme are:

$$N_2 \leftrightarrow 2N$$
$$O_2 \leftrightarrow 2O$$
$$H_2 \leftrightarrow 2H$$
$$O_2 + H_2 \leftrightarrow 2OH$$
$$O_2 + 2CO \leftrightarrow 2CO_2$$
$$O_2 + 2H_2O \leftrightarrow 4OH$$

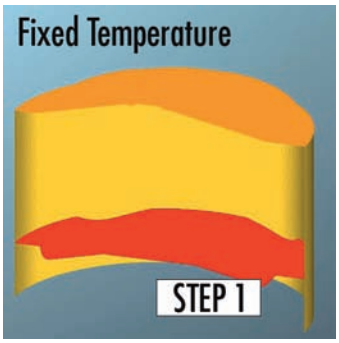

WALL	T/Tref
Piston	1
Intake Valve	0.853
Exhaust Valve	0.853
Head	0.853
Liner	0.79

Fig. 3: Imposed wall temperature in the first step.

A preliminary calibration of the model of turbulent combustion is needed. A robust reference for the combustion evolution comes from the analysis of the pressure evolution inside the chamber in the particular configuration analyzed with high thermal loads. The Han and Reitz law at the wall has been used for the evaluation of the heat flux: the model takes the change in gas density into consideration. The initial conditions are mapped from the results of intake simulations, whereas the wall temperature is more difficult to estimate. The most common procedure is to assign uniform wall temperature to each component in the combustion chamber, based on experience or from information in the literature review.
The accurate estimation of the wall temperature distribution is the main goal of the integrated CFD/FEM methodology, thus an iterative procedure for the definition of heat flux and temperature has been used. Combustion simulations allow extracting thermal fluxes at the wall, which are used in FEM simulations as boundary conditions. This iterative cycle is accomplished since the wall temperatures estimated by FEM in a defined cycle are equal to those of the previous cycle. Fig. 3 shows the non-dimensional temperatures imposed in the first cycle (Tref is the piston temperature imposed as a first attempt).
The results of the combustion simulation are validated against experimental data provided by Ducati: the simulated pressure traces in the chamber are compared with those obtained on the test bench, allowing the calibration of the models for the correct representation of combustion velocity.
CFD simulations cannot correctly reproduce the recovery of tolerance and the deformation of the piston rod and the crankshaft, thus the volume of the chamber at TDC (Top Dead Centre) is lower than in reality, leading us to maintain a gap in the peak pressure as shown in Fig. 4. This overestimation of the pressure has no effect on the evaluation of the heat flux, because the real internal energy of the gas is hidden

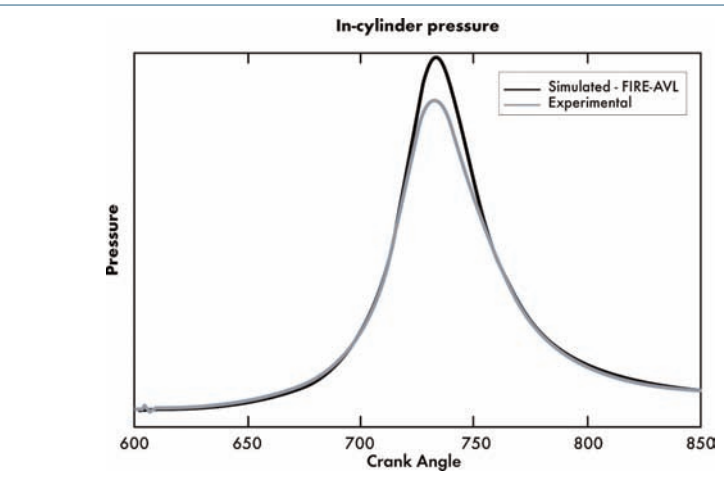

Fig. 4: In cylinder pressure during combustion (step 1).

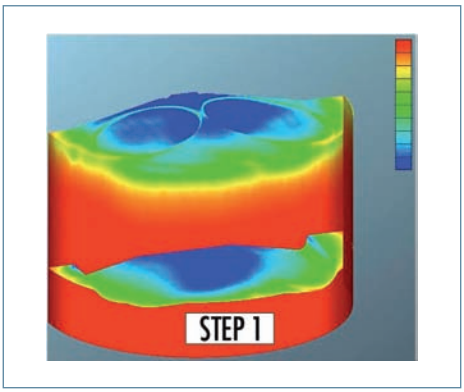

Fig. 5: Mean heat flux map extracted at the wall.

by the real higher volume of the chamber compared to that of the theoretical rigid piston movement.
At the end of this first CFD simulation the heat fluxes, averaged over the engine cycle, are extracted at the wall (Fig. 5) and a new iteration cycle with FEM simulation starts.

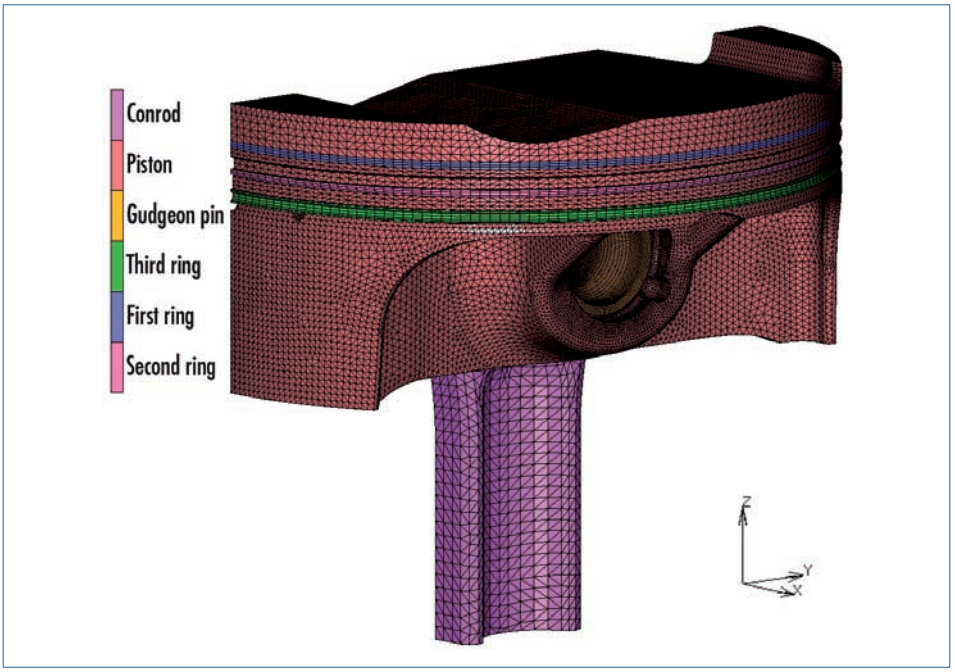

Fig. 6: Finite Element model.

FEM ANALYSIS – CALCULATION OF THE TEMPERATURE FIELD INSIDE THE PISTON

FEM MODEL

In order to estimate the temperature field inside the piston, a Finite Element model has been created which includes the discretization of the piston, the piston pin, and the upper portion of the conrod (Fig. 6). Because of the symmetric aspect of the problem, only half of the whole structure has been modelled, with consistent advantages in terms of modelling and the computational time saved. The Finite Element model consists of about 450000 elements and 180000 nodes.
The FEM commercial software MSC.Marc/Mentat2007r1 has been employed.

BOUNDARY CONDITION

The boundary conditions applied to the different parts of the model are described below.
Piston crown
In the Finite Element model, the results from the CFD combustion analysis previously described are employed as external boundary conditions and are properly applied to the top surfaces of the piston, which make up part of the combustion dome (Fig. 7).

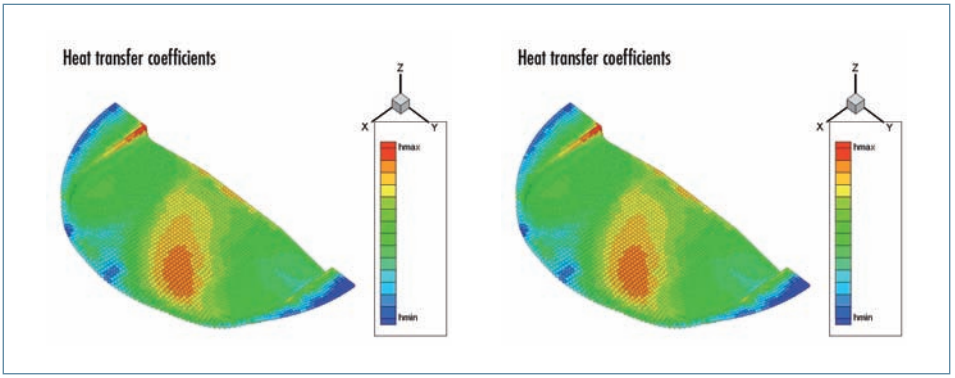

Fig. 7: Boundary condition applied to top surfaces of the piston.

Considering the calculation of the thermal diffusion inside the piston is usually performed in a stationary regime [1], instantaneous heat transfer coefficients and gas temperatures deriving from the CFD combustion analysis are correctly averaged through a single thermodynamic cycle of the engine (Fig. 7).
Once the boundary conditions applied to the upper surfaces of the piston have been defined, the thermal energy the piston exchanges with the other components, and with the oil, has to be estimated in order to solve the problem of the thermal diffusion inside the piston.
Starting from bibliographic results [3], various formulae, of both analytical and empirical derivation, have been identified allowing the different heat transfer coefficients to be estimated as a function of various engine parameters.
As a consequence, the piston has been subdivided into a certain number of zones and proper values of heat transfer coefficients and reference temperatures have been estimated for each zone.

Piston rings
The following assumptions have been made to estimate the heat transfer in the ring land [1]:

- the effect of the motion of the piston on the heat transfer is neglected;
- the rings are fully engulfed in oil and no cavitation occurs;

- the rings do not twist;
- the only heat transfer mode in the oil film is assumed to be conduction.

The thermal circuit method has then been employed to mimic the heat transfer mechanism (Fig. 8), with:

- R_1 - conductive oil film resistance;
- R_2 - conductive liner resistance;
- R_3 - convective water-jacket resistance [1].

For each ring, a heat transfer path is considered (Fig. 8) and the values of R_1, R_2, R_3 are calculated.

The effective heat transfer coefficients are obtained from:

$$h_{eff} = \frac{1}{R_{tot} A_{eff}}$$

where R_{tot} is the total resistance and A_{eff} is the effective contact area between each ring and the liner.

Table 1 properly summarizes the adimensionalized values of heat transfer coefficients and reference temperatures, calculated for the three rings.

Table 1. Boundary conditions applied to rings.

	Heat transfer coefficient	Reference temperature
I ring	1	1
II ring	0.654	1
III ring	0.385	1

Piston skirt

To evaluate the heat transfer coefficient in the skirt zone (Fig. 9), the same assumptions introduced for the ring land have been adopted. Table 2 properly summarizes adimensionalized values of the heat transfer coefficient and reference temperature.

Table 2. Boundary conditions applied to the piston skirt.

	Heat transfer coefficient	Reference temperature
Piston skirt	0.423	1

Underside zone of the piston crown

The underside zones of the piston are wetted by the oil in the engine carter. In order to improve the cooling performance, an oil jet hits the underside zone of the piston crown directly in the point shown in Fig. 10.

While the other parts of the underside area are simply splashed with the oil that is centrifuged by the crankshaft rotation. As a consequence, the heat transfer coefficient in the area directly hit by the oil jet is different from the heat transfer coefficient in the other parts that have simply been splashed by the crankshaft rotation. Moreover, horizontal and vertical underside zones have to be distinguished. In conclusion, different areas have to be identified in order to correctly define the heat transfer mechanism in the underside zone of the piston that has been splashed with oil (Fig. 11).

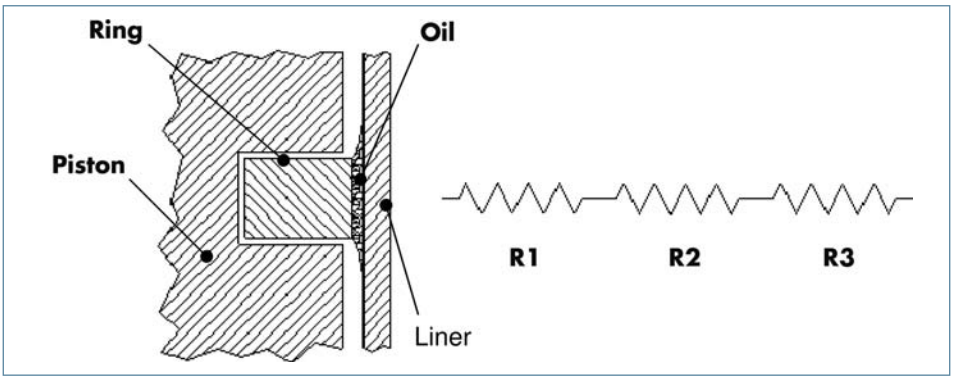

Fig. 8: Thermal resistance model of the rings.

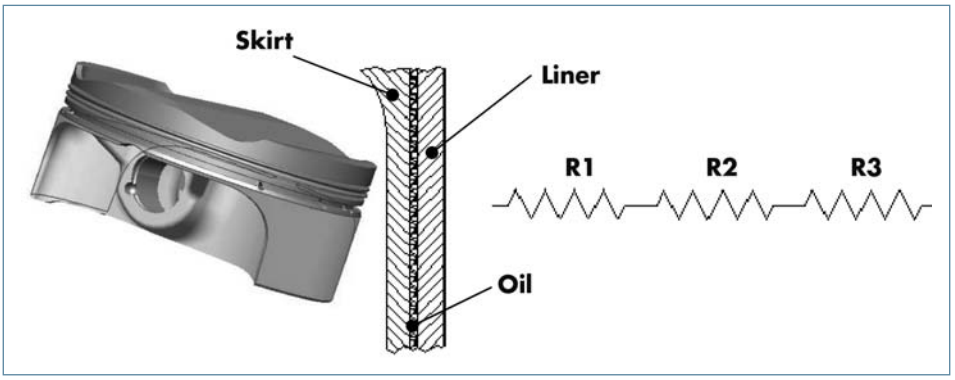

Fig. 9: Thermal resistance model of the piston skirt.

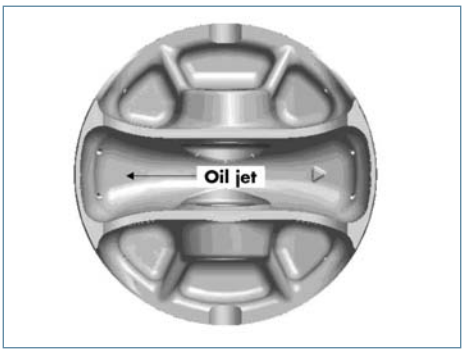

Fig. 10: Underside zone of the piston crown.

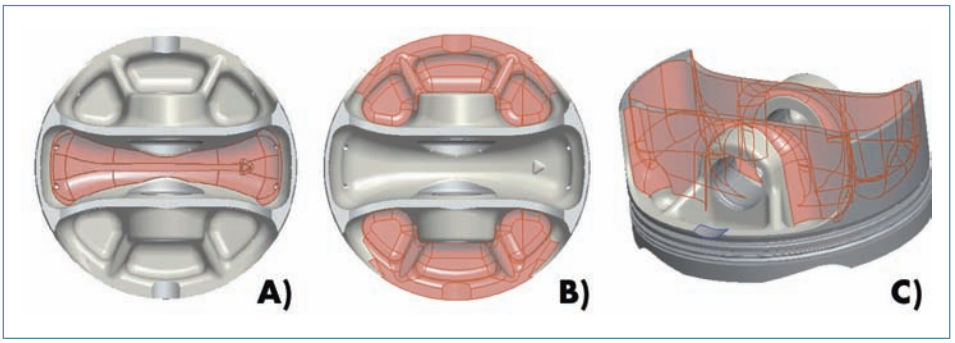

Fig. 11: – a) oil jet, b) underside horizontal surfaces, c) underside vertical surfaces.

Starting from empirical and analytical bibliographic results [1,3,5], proper heat transfer coefficients have been calculated for the different zones of Fig. 11. Table 3 correctly summarizes the adimensionalized values of the heat transfer coefficients and reference temperatures, calculated for the underside areas of the piston crown.

Table 3. Boundary conditions applied to the different zones of Fig. 11.

	Heat transfer coefficient	Reference temperature
Zone a)	0.288	1.22
Zone b)	0.088	1.22
Zone c)	0.016	1.22

Conrod and gudgeon pin

The same heat transfer coefficient calculated for the vertical surfaces of the underside area of the piston crown has been applied to the externals surfaces of the conrod and gudgeon pin (Table 4).

Table 4. Boundary conditions applied to the conrod and gudgeon pin.

	Heat transfer coefficient	Reference temperature
Conrod and gudgeon pin	0.016	1.22

RESULTS

Fig. 12 shows the thermal field calculated inside the piston, once the data exchange procedure between the CFD and FEM analysis has reached convergence.

As expected, the maximum temperature falls at the top surface of the piston crown. Interestingly, this peak of temperature does not occur at the centre of the piston where the highest gas temperatures exists, but is shifted towards the perimetrical zone. This is related to the higher cooling capabilities of the oil jet that directly hit the central area underneath the piston.

CFD ACTIVITY – COMBUSTION STEP 2

In the second step of the CFD simulation, the wall temperature is imposed with a non-uniform spatial distribution, as resulting from the thermal diffusion analysis inside the components given by the previous FEM step (Fig. 13).

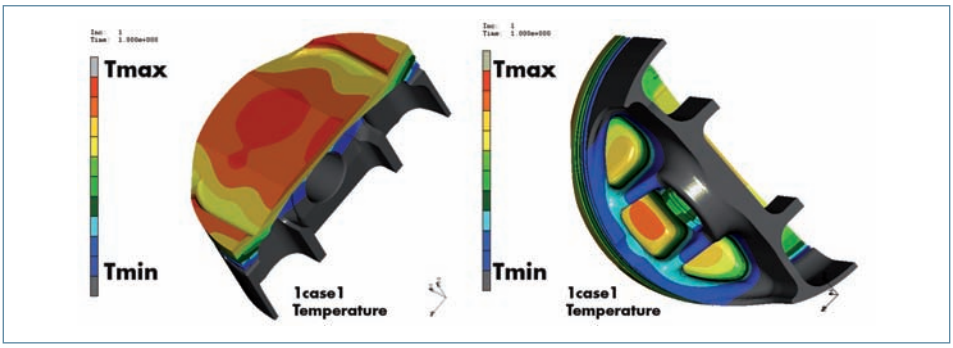

Fig. 12: Thermal field inside the piston.

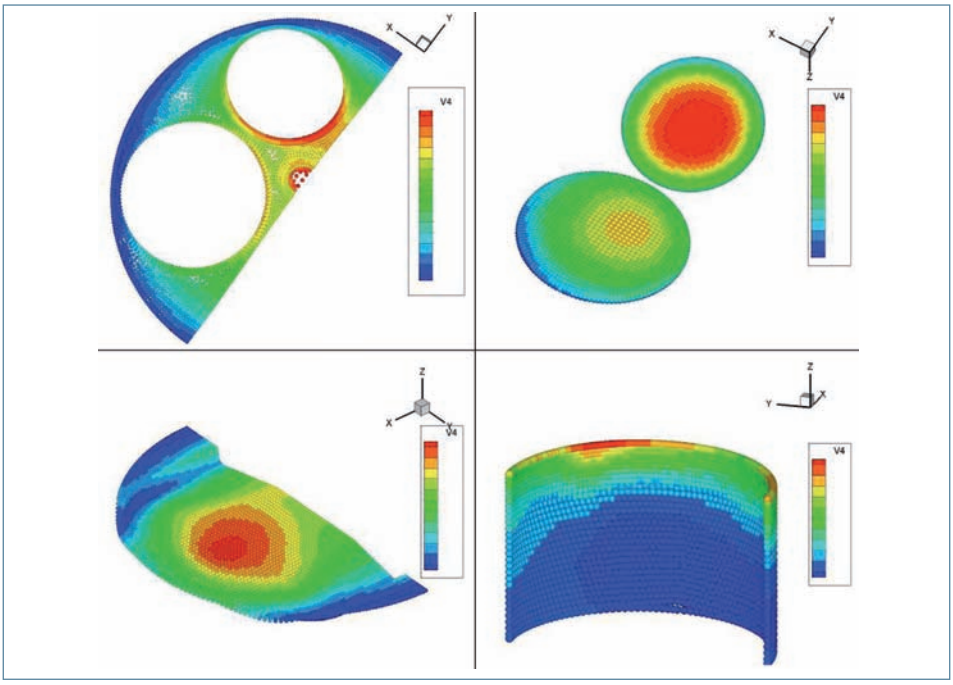

Fig. 13: Spatial distribution of temperature of each component part (step 1).

Analysis of the new boundary conditions shows a consistent difference in the mean temperature values of the FEM analysis compared to those of first attempt, only for the intake and exhaust valves (Fig. 14).

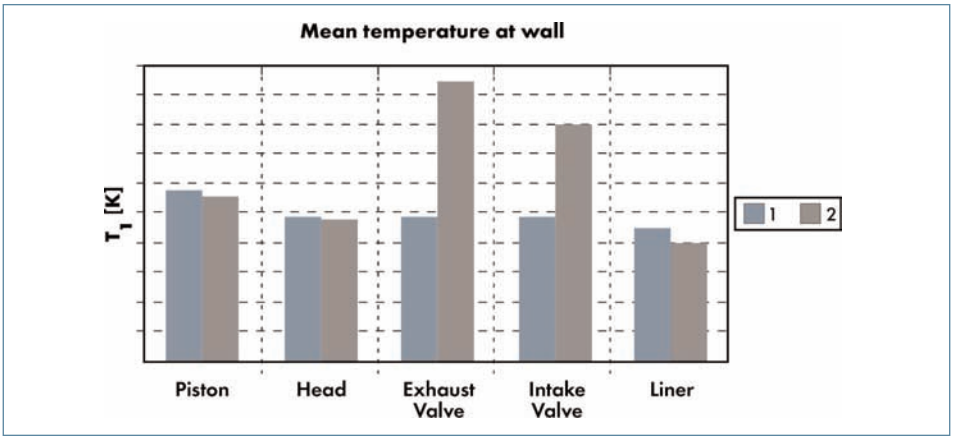

Fig. 14: Mean surface temperature of each component part for step 1 and step 2.

The new boundary condition causes a change in the combustion speed. The early stages of combustion are accelerated by the wall surface close to the spark plug that is hotter than the first step, while the end of combustion is slower because of the colder temperature of the peripheral zones of the combustion chamber. As a consequence, new calibration of the CFD combustion model is needed, in order to obtain the right pressure evolution with respect to the experimental one. The final result is shown in Fig.15, where the new red curve is superimposed onto that of the first cycle with uniform imposed temperatures (green line).

The new boundary condition causes a change in the evaluation of the wall thermal load and a new spatial distribution of the heat flux on the different surfaces. A general reduction in the heat transferred to the wall has been observed, of about 11% (Fig. 16).

It can be noted in Fig. 16 that the heat flux adjusts to the new boundary conditions by increasing the total amount of energy transferred at the wall in the coldest zones. The variation of the thermal flux at the wall is clear in the analysis of the result of the second step of the CFD simulation (Fig. 17). It is interesting to notice the extremely consistent change in the valves compared to the remaining part of the combustion chamber.

The methodology for the evaluation of the thermal load on the wall reaches a converged result only in two cycles. The importance of the evaluation of the heat flux and the difference in the amount of energy estimated in the first and the second cycle shows the needs for application of such an iterative procedure.

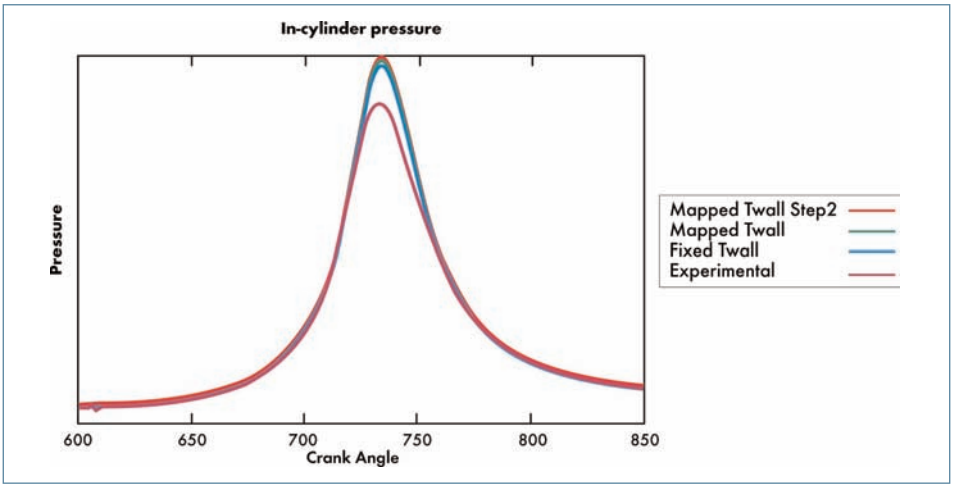

Fig. 15: Comparison of pressure traces with different wall temperature conditions (step 2).

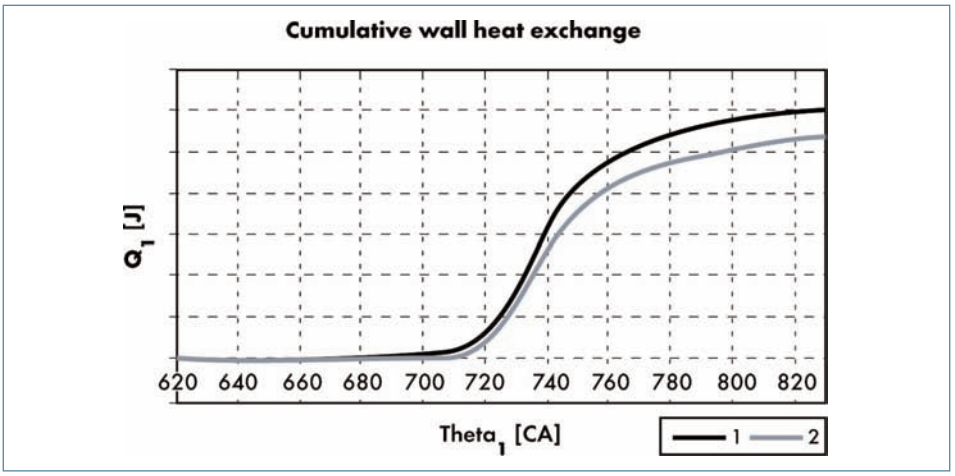

Fig. 16: Cumulative heat exchange at wall.

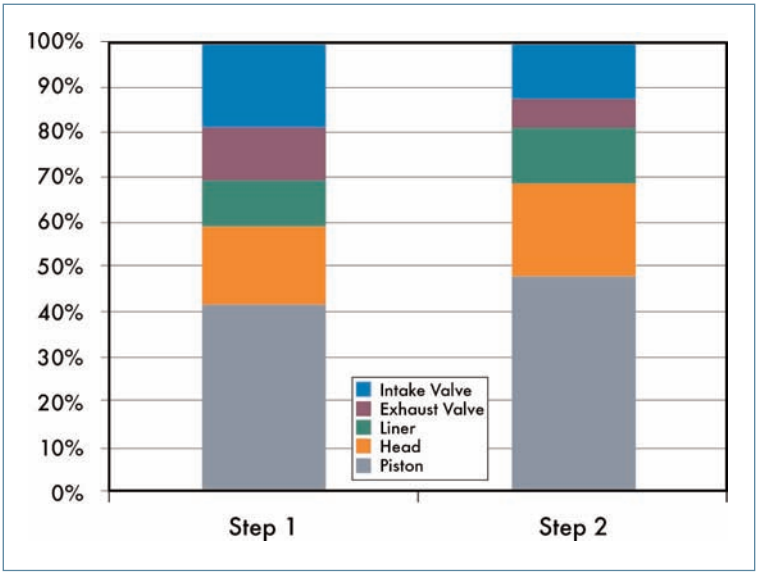

Fig. 17: Distribution of heat flux at the wall.

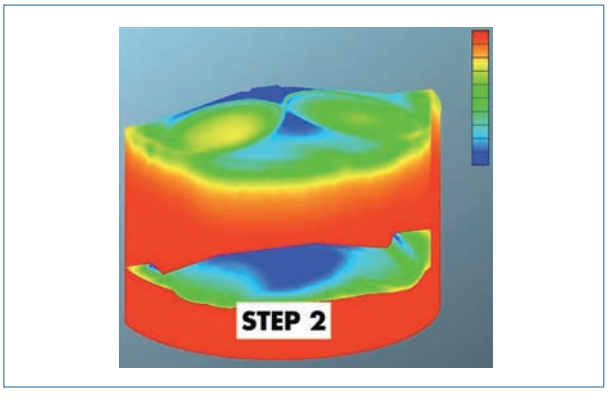

Fig. 18: Mean heat flux map at the wall – Step 2.

VALIDATION OF THE MODELS

The precipitation hardening aluminum alloys reach peak hardness after the T6 heat treatment, which includes: solubilization and quenching, followed by artificial aging. It is well-known, however, that they can exhibit a strength loss after exposure at temperatures close to, or higher than the aging temperatures, for a given time.

This reduction in the mechanical strength is due to the overaging of the Al alloy induced by coarsening of the reinforcing precipitates and can be evaluated by means of hardness measurements, since its variation depends on temperature and exposure time.

The knowledge of the curves of the hardness variation of the alloy exposed at a high temperature for different times, allows an estimation of the temperature reached by a mechanical component, through the knowledge of its residual hardness at a given temperature for a fixed time.

In order to obtain reliable results it is very important to verify the following: (a) the hardness curves as a function of temperature and time are accurately identified for the alloy, subjected to the same process condition and heat treatment as the component under investigation; (b) the control of the component microstructure, before and after testing, to make sure that possible hardness variation is not related to other microstructural modifications, such as, for example, grain growth, rather than overaging [6-9].

MATERIAL AND EXPERIMENTAL PROCEDURE

The pistons under investigation were made with the 2618 aluminum alloy, of which the chemical composition is given in Table 5.

They were produced by forging and therefore were heat treated to the T6 condition. The heat treatment included: a multiple step solubilization treatment in a furnace pre-heated to 200°C, with heating at 495°C for 1.5 h, followed by fast heating at 507°C and 3 h soaking, a subsequent fast heating at 525°C and soaking for 8 h; water quenching (60-90°C); and artificial aging at 200°C for 20 h.

The chemical composition of the alloy allows the increase of the high temperature strength of the alloy thanks to the presence of Ni and Fe, but operating temperatures close to, or higher than the aging temperature, can lead to loss in the mechanical strength due to overaging.

The hardness curves as a function of temperature and time (TTH curves) for the AA2618 were obtained by heating different specimens at various temperatures (in the range 200-305°C) and for different times (from 2 min to 7 days), followed by water quenching. Samples (6x5x3 mm^3) were cut from the crown of the forged pistons, heat treated to T6 condition; before heating in the furnace, the samples were polished in order to perform more accurate hardness measurements. Two samples for each temperature and time condition were prepared and 3 Brinell hardness tests were performed on each sample, according to ASTM E 10-08 [10], by means of a martensitic steel ball (Φ=2.5 mm) under an applied load of 62.5 kg.

The microstructural characterization of the alloy was carried out by optical microscopy with an image analyzer, on specimens cut from different zones of the piston and prepared according to standard metallographic procedures (ASTM E3 [11]). In order to reveal the grain boundaries, the specimens were electrochemically etched with Barker's solution (5 mL HBF4 (48%) in 200 mL water) and were anodized for about 80s under 15 V, according to ASTM E 883 [12].

Table 5. Nominal chemical composition (wt%, min e max) of the 2618 aluminum alloy

Si	Fe	Cu	Mn	Mg	Zn	Ti	Ni	Zr	Bi	Ni	Pb	Sn	Cr	Al
0.150	0.900	1.800	0	1.200	0	0	0.800	0	0	0.080	0	0	0	Bal
0.250	1.400	2.700	0.250	1.800	0.150	0.200	1.400	0.050	0.050	1.400	0.050	0.050	0.050	

RESULTS

The variation of the hardness as a function of temperature and time for the 2618 Al alloy is reported in the TTH curves in Figs19-20.

The microstructural analyses of the forged and T6 heat treated pistons showed a fully recrystallized microstructure (Fig. 21). Different grain sizes were measured in different zones of the piston, probably due to the different deformation conditions imposed on the component during the forging process.

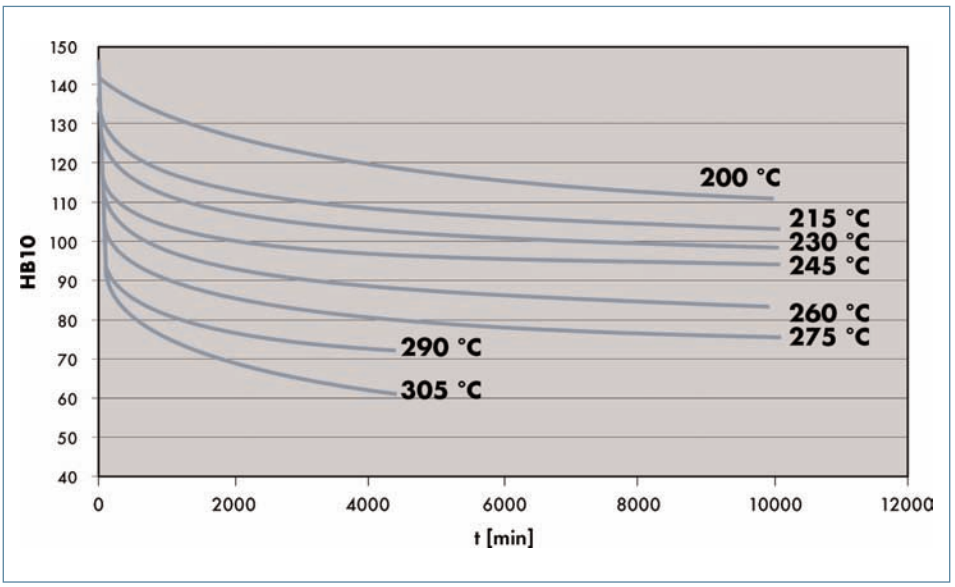

Fig. 19: Hardness variation of the T6 heat treated 2618 Al alloy after exposure at various temperatures (ranging from 200 to 305°C) for different times (from 2 min to 7 days).

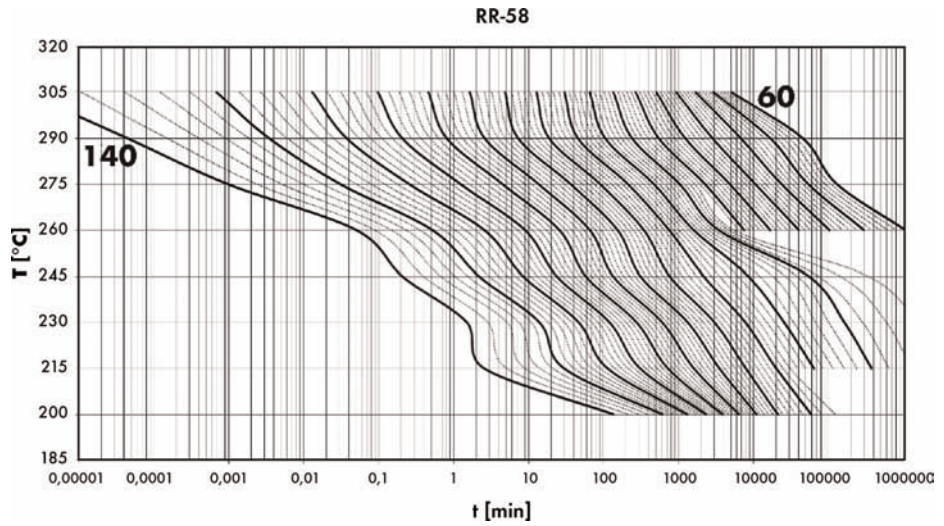

Fig. 20: Temperature required to attain a particular value of Brinell hardness (between 60 and 140 HB) as a function of time for the T6 heat treated 2618 Al alloy (TTH curves).

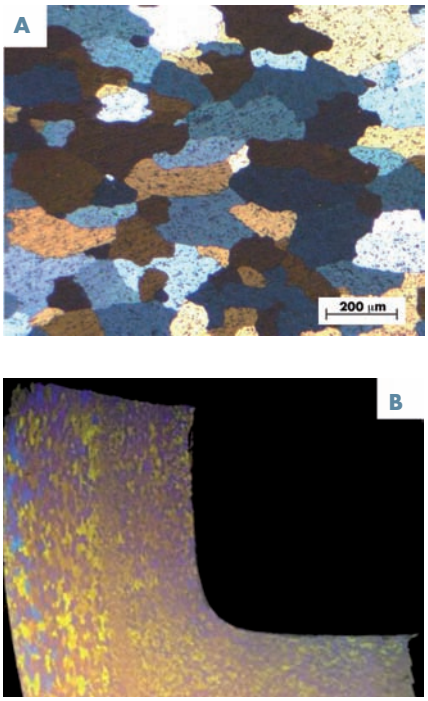

Fig. 21: Optical micrographs of piston crown under polarized light, showing: recrystallized grains (a), section of the piston with grains of different size in zones subjected to different forging conditions (b).

Similar microstructural features were found in the pistons after bench testing, making it reasonable to assume that the observed changes in alloy hardness are simply the consequence of overaging.
This allows the use of TTH curves for assessment of temperatures reached in different parts of the component.
The hardness measurements performed on the piston crown before testing gave hardness values between 141 and 145 HB10, while after 27 hours of bench testing a hardness reduction was observed between 101 to 115 HB10, in different zones of the piston crown, as shown in Fig. 22.
By using the TTH curves in Fig. 20, giving the running time of the engine and the hardness measured on the piston as input data, it was possible to obtain a map of the temperatures reached in various parts of the piston (Fig. 22) which, compared with those obtained through FEM analysis (Fig. 23), show very good correspondence, with a maximum variation of a few degrees, and confirm the validity of the proposed methodology.

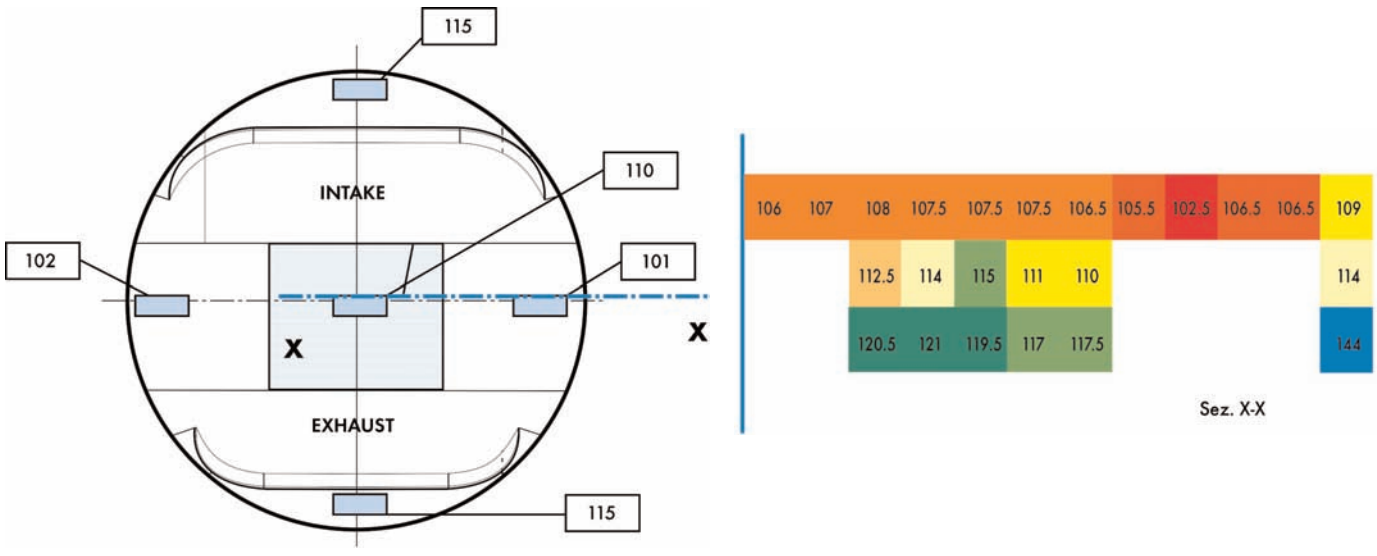

Fig. 22: Hardness values (HB10) measured in the central section X-X of the piston crown at 2 mm depth. The temperatures evaluated from hardness data in Fig. 20, reached in the section X-X, are indicated.

CONCLUSIONS

A multidisciplinary approach was applied for the development of an integrated methodology for the design of aluminum alloy pistons used in high performance internal combustion engines in motorcycles. The research particularly focused on the development of an advanced CFD/FEM simulation methodology, for the correct prediction of the thermal diffusion inside the piston, with subsequent validation of the results obtained through microstructural characterization and hardness measurements. The model used in the FEM analysis of the thermal diffusion, received the combustion analysis results as input. The transfer of the thermal load from CFD models to FEM models was optimized by applying a combination of thermal exchange coefficients and spatially variable gas temperatures on the top surface of the piston. The results of the FEM simulations were validated by the estimation of the local temperatures of the component, partly performed by means of the hardness curves of the T6 heat treated AA2618 alloy used for the pistons, as a function of temperature and time, obtained experimentally by means of lab tests carried out according to the required temperature and time conditions.

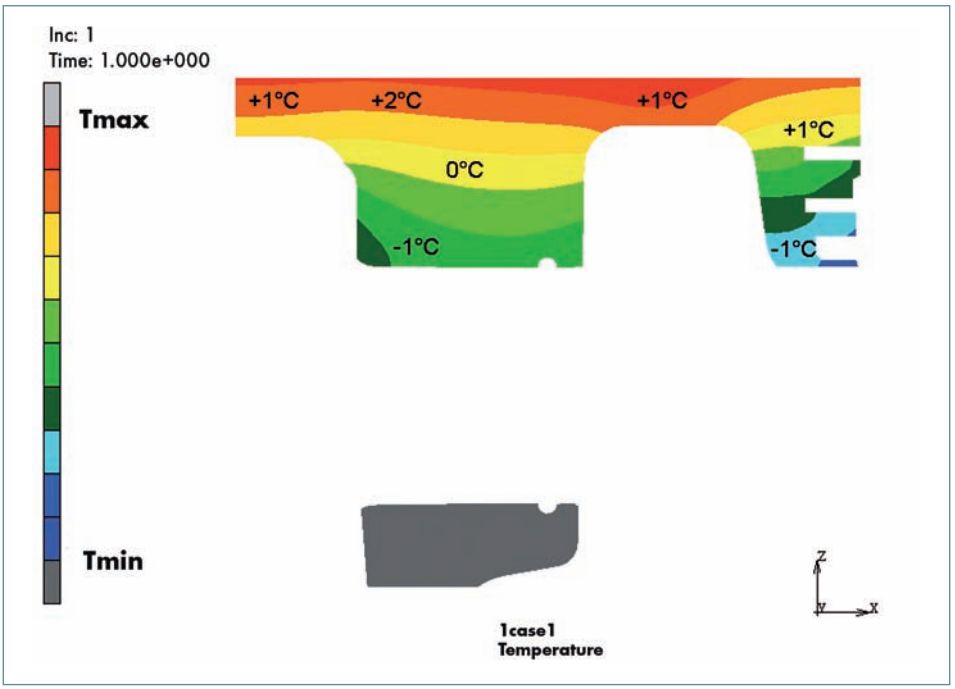

Fig. 23: Differences between temperature values obtained by FEM simulation and those estimated by the hardness tests in section X-X of Fig. 22.

ACKNOWLEDGEMENTS

This research activity was carried out as part of the FIRB RBIP068WAA project, funded by the MINISTRY OF EDUCATION, UNIVERSITY AND RESEARCH and by the DIMEC and DIEM departments of University of Modena & Reggio Emilia and University of Bologna respectively.
The authors would like to thank Ducati Motor Holding SpA for their support.

REFERENCES

[1] V. Esfahanian, A. Javaheri, M. Ghaffarpour, Appl Therm Eng., 26, 2006, pp. 277-287.
[2] Colin O., Benkenida A., Angelberger C. Rev. IFP, 58,1, 2003, pp. 47-62.
[3] Furuhama, H. Suzuki. Bullettin of the JSME, 22, 1979, pp. 174-182.
[4] H. W. Wu, C. P. Chiu. Computers & Structures, 1989, 325, pp 997-1004.
[5] C.D. Rakopoulos, G.C. Mavropoulos, D.T. Hountalas. SAE, Intern. Congress and Exposition, Cobo Center, Detroit, Michigan, U.S.A., SAE Paper No 981024.
[6] Jianhua Wang, Danqing Yi, Xuping Su, Fucheng Yin. Mat. Char., 59, 2008, pp. 965–968.
[7] F. Novy, M. Janecek, R. Král. J Alloys Compd, 487, 2009, pp. 146–151.
[8] Pier Gabriele Molari, Piero Morelli, Sergio Maldotti and Tito Poli. Key Eng. Mat. 324-325, 2006, pp. 1095-1098.
[9] Y. Leng, W.C. Port, Jr. and R.P. Gangloff. Scripta Met. et Mat., 24, 1990, pp. 2163-2168.
[10] ASTM E 10-08 (2007) Standard Test Method for Brinell Hardness of Metallic Materials 1
[11] ASTM E3-01 (2007) Standard Practice for Preparation of Metallographic Specimens
[12] ASTM E883-02 (2007) Standard Guide for Reflected–Light Photomicrography